Astron. Astrophys. 341, 275–285 (1999)

ASTRONOMY
AND
ASTROPHYSICS

Radiation scattering in the solar corona

G. Noci and L. Maccari

Dipartimento di Astronomia e Scienza dello Spazio, Università di Firenze, Largo Fermi 5, I-50125 Firenze, Italy

Received 4 December 1997 / Accepted 31 July 1998

Abstract. This paper discusses the scattering in the solar corona of the radiation emitted by the solar disk. We obtain expressions for the emissivity which permit to deduce the spectral characteristics of the scattered radiation. With these expressions, assuming a Maxwellian distribution for the velocities of the scattering ions and a simple spectral shape of the exciting radiation, we produce approximate analytic formulae which show some interesting properties of the scattered radiation that do not clearly emerge from the exact expressions. Among them, the expression for the Doppler shift of the radiatively excited component of a line, and that for its width. We also examine the case of bi-Maxwellian velocity distributions and the scattering by the free electrons.

Key words: scattering – line: profiles – Sun: corona – Sun: UV radiation

1. Introduction

The scattering of the photospheric radiation by the free electrons of the solar corona has been studied in the past by a number of authors, who elaborated a method to determine the electron density from measurements of the polarized brightness in the visible continuum, obtained in eclipse (van de Hulst 1950). Later on, a method for the determination of the same quantity from coronagraphic observations has been presented by Altschuler & Perry (1972). The spectral shape of the scattered radiation has been the object of the work of van Houten (1950), who analyzed the effect of the electron scattering on the profile of the absorption lines in the visible spectrum, and of Hughes (1965), who calculated the profile of the electron scattered Lyα.

Scattering of disk radiation is also operated by ions in discrete transitions. Indeed, the most intense coronal line, Lyα, is due to such a process (Gabriel et al. 1971). The study of this process (resonant scattering) has been initiated by Hyder & Lites (1970), who analyzed the brightening and dimming effects in the Hα and Lyα lines due to the neutral hydrogen atoms present in moving clouds above the photosphere, with particular reference to an eruptive prominence. Expressions for the profile of the resonantly produced Lyα line have been given by Beckers & Chipman (1974), Kohl & Withbroe (1982), Withbroe et al. (1982), who also gave an expression for the component of this line due to the scattering by the free electrons, and Olsen et al. (1994). Noci et al. (1987) analyzed the properties of the coronal O VI resonance doublet, which is produced, in part, by resonant scattering.

Observations of profile and total intensity of Lyα and other lines produced in the solar corona by scattering of the chromospheric or transition region radiation, very scanty in the past, are now accomplished routinely by the SOHO instruments, in particular by the UVCS (Ultraviolet Coronagraph Spectrometer). This instrument observes, in its normal mode of operation, at heliocentric distances larger than $\simeq 1.5 r_\odot$, where the density is low enough to make the collisional excitation of some UV lines of the same order, or smaller, than the radiative excitation. Among them, the H I lines of the Lyman series and the ion lines arising from the $2s - 2p$ transitions of the Li isoelectronic sequence (Withbroe et al. 1982). Also the measurement of the profile of the electron scattered Lyα, very difficult because the line is much less intense ($\lesssim 10^{-3}$) than the resonant component, and, furthermore, much broader (FWHM $\gtrsim$ 40 Å), is within the capabilities of the UVCS instrument (Kohl et al. 1997). Its achievement is very important because it would lead to a direct determination of the electron thermal speed.

A numerical integration which involves the spectral shape of the exciting chromospheric or transition region radiation is needed to calculate the scattered intensity. Some important characteristics of it, like, for instance, the amount of shift, by Doppler effect, of a scattered line, can not be easily deduced from the expressions which exist in the literature. The purpose of this paper is to express the emissivities, both for the resonant and electron scatterings, with simple expressions by means of an appropriate choice of the axes in the velocity space, where the velocity distribution function of the scattering particles is defined. These allow an easy production of approximate forms, which not only permit rapid, first approximation calculations, but also, which is more important, show the main characteristics of the coronal scattered radiation, and are therefore very useful for the interpretation of the observations.

The accuracy of these formulae will be discussed and comparisons with numerical integrations will be reported.

Send offprint requests to: G. Noci, (gnoci@arcetri.astro.it)

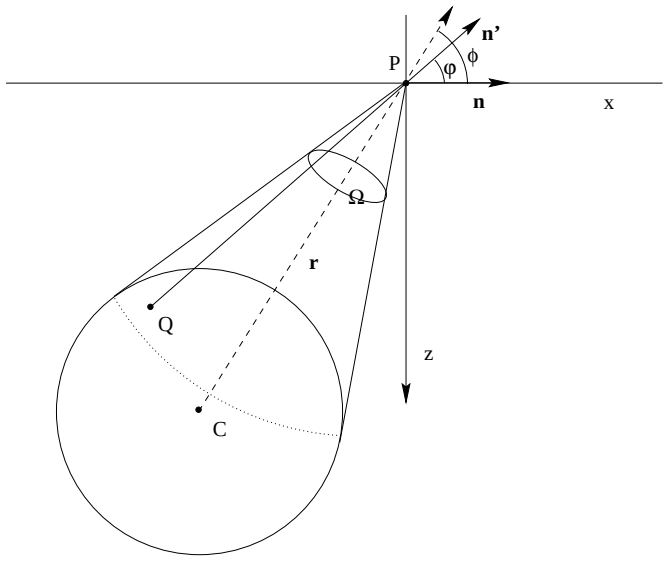

Fig. 1. Scattering process at the coronal point P (**r**= radial direction, $\mathbf{n}'$= direction of incoming radiation, **n**= direction of scattered radiation, i.e. line of sight). The axis Z is in the **r, n** plane.

Our analysis follows an approach quite similar to that of Beckers & Chipman (1974), for the resonant scattering produced by neutral hydrogen and other ions, considering, however, their assumption of point source only as a particular case. For the scattering due to the free electrons we follow the approach of van Houten (1950). Like these authors, we assume that the frequency of the scattered photon does not change, during the process, in the frame where the scattering particle is at rest.

2. Scattering by ions

We start with the discussion of the scattering operated in a discrete transition and we focus our attention on the resonance lines, so that we will not include any branching coefficient in the expressions. The formulae for the emissivity that we will derive, however, can be easily extended to other lines, such as Lyβ, by taking such coefficients into account.

2.1. Line profile

We consider the absorption of a photon moving in the direction $\mathbf{n}'$ by an ion at the coronal point P, with velocity $\mathbf{v}$, followed by its re-emission in the direction **n** (Fig. 1). This process is described by the Einstein coefficient B_{12} relative to the transition considered and a geometrical factor, $p(\varphi)$, which represents the probability for the absorbed photon to be deflected through the angle φ. The emissivity due to this scattering process, at the frequency ν (for the Earth observer), can be written as:

$$j(P,\nu,\mathbf{n}) = \frac{chB_{12}N}{4\pi}\int_\Omega p(\varphi)d\omega' \times \tag{1}$$

$$\int_{-\infty}^{\infty} I(\nu'[v_X(\nu),v_Y,v_Z,\nu_o],\mathbf{n}')f(v_X(\nu),v_Y,v_Z)dv_Y dv_Z,$$

where h is Planck's constant, c the speed of light, N the number density of the absorbing ions, $f(v_X,v_Y,v_Z)$ their velocity distribution function, ν_o the frequency of the transition, ν' that of the absorbed photon for the observer at rest, $I(\nu',\mathbf{n}')$ the intensity of the disk radiation arriving at P along the direction $\mathbf{n}'$ (i.e. from the point Q, Fig. 1), and we have taken a Cartesian system with the origin in P, the X axis along **n** and the Z axis in the $\mathbf{n},\mathbf{r}$ plane (Fig. 1), being **r** the vector from the center of the Sun to the point P. The Z axis is directed towards the Sun. This equation expresses the fact that the frequency of emission and that of absorption are the same (ν_o) for the absorbing atom, while they are ν and ν', respectively, for the Earth observer. With the coordinate system chosen here, ν depends on the velocity component v_X only, while ν' depends on all three velocity components, namely:

$$\nu = \nu_o(1+\frac{v_X}{c}) \tag{2}$$

and

$$\nu' = \nu_o(1+\frac{v_{n'}}{c}), \tag{3}$$

being $v_{n'} = \mathbf{v}\cdot\mathbf{n}'$ (relativistic effects can be neglected for particles of the solar corona). The scattering factor $p(\varphi)$ has the form

$$p(\varphi) = \frac{1}{8}\frac{7+3\cos^2\varphi}{4\pi}$$

for a ${}^2S_{1/2} - {}^2P_{3/2}$ transition,

$$p(\varphi) = \frac{1}{4\pi}$$

for a ${}^2S_{1/2} - {}^2P_{1/2}$ transition and

$$p(\varphi) = \frac{1}{12}\frac{11+3\cos^2\varphi}{4\pi}$$

when the two lines corresponding to these transitions are not resolved, as in the case of the solar Lyα line (Chandrasekhar 1950; Landi Degl' Innocenti 1984).

Eq. (1) extends the one given by Beckers & Chipman (1974), to include the case of a source of radiation which is not a point. It assumes that the width of the absorption profile of the ion (due to natural and collisional broadenings) is negligible compared with the width of the exciting line, and that also multiple scatterings are negligible. The first assumption is certainly valid for the thin coronal gas; as for the second, we can make easily an order of magnitude estimate: the probability, for a photon of a spectral line, at the coronal point P, to be scattered before its exit from the corona is roughly equal to the ratio between the coronal brightness on the line of sight through P and the disk brightness, and this ratio gives, approximately, not only the probability of single scattering but also that of multiple to single scattering. Its value is, for the Lyα line, $\sim 10^{-3}$ at the coronal base in a streamer (Gabriel et al. 1971), $\sim 3\times10^{-5}$ at $r = 1.7r_\odot$ in an active region streamer (Raymond et al. 1997). For lines of ions more abundant than H I the ratio can be larger.

For example, for the O VI 1032 Å line it is ten times more than for Lyα at $r = 1.7 r_\odot$, according to Raymond et al. (1997). If the O VI to H I abundance ratio remains the same at the coronal base, we get, there, for the O VI 1032 Å line, the value $\simeq 10^{-2}$ for the ratio between coronal brightness (radiative component) and disk brightness. In other words, even for lines of sight close to the disk, multiple scattering is only a 10^{-2} effect for the O VI resonance lines. Other ions (Mg X, Si XII, Fe XII) are presumably more abundant than O VI, but the transition coefficients (B_{12}) of their resonance lines are lower, so that we do not expect a situation very different from O VI. We conclude that multiple scattering is a negligible effect in the solar corona.

Eq. (1) is the basic equation for the emissivity of a radiatively excited line. The calculation of it needs numerical integrations once the exciting intensity, which can be different from one direction $\mathbf{n}'$ to another, and the velocity distribution function are specified.

Finally, the scattered intensity is obtained from the emissivity by integration along the line of sight (**n**):

$$I_S = \int_{-\infty}^{\infty} j(P, \nu, \mathbf{n}) dX. \tag{4}$$

For what concerns the velocity distribution function of the absorbing ions, let us consider, as examples, two possibilities: the first one characterized by the fact that the radial component of the velocity, $v_\parallel = \mathbf{v} \cdot \mathbf{r}$, has a different distribution from that of the perpendicular component, $v_\perp$, both distributions being Maxwellian; as a second example we consider a purely Maxwellian distribution. In the former case

$$f = \frac{1}{(\pi)^{3/2} V_\parallel V_\perp^2} \exp(-[v_\parallel - w_\parallel]^2/V_\parallel^2 - v_\perp^2/V_\perp^2),$$

where $V_\parallel = \sqrt{2kT_\parallel/m}$ and $V_\perp = \sqrt{2kT_\perp/m}$, being k the Boltzmann constant, m the ion mass and $T_\parallel, T_\perp$ the parallel (radial) and perpendicular kinetic temperatures, respectively, and the solar wind velocity **w** has been assumed in the radial direction. Hence Eq. (1) will be numerically calculated taking into account the transformations

$$v_\parallel = v_X \cos\phi - v_Z \sin\phi$$

$$v_\perp = \sqrt{(v_Z \cos\phi + v_X \sin\phi)^2 + v_Y^2},$$

where ϕ is the angle between **n** and **r** (Fig. 1). In other words, for any v_X, v_Y, v_Z one obtains f from the above equations and ν', and thus I, from Eq. (3).

The situation is much simpler in the latter case (Maxwellian distribution), since this distribution function can be factorized in three unidimensional Maxwellian distributions for any choice of the axes. (As a matter of fact it is sufficient, for what follows, that the factorization property of the velocity distribution function hold for rotation around the X axis.) In this case the scattering process can be described by taking, as above, one axis, the x axis, along **n** ($x \equiv X$), but having the z axis in the $\mathbf{n}, \mathbf{n}'$ plane, towards the Sun. In this reference frame $v_{n'}$ is a function of two velocity components only,

$$v_{n'} = v_x \cos\varphi - v_z \sin\varphi, \tag{5}$$

and so is ν' (Eq. (3)). Since ν', and thus the exciting intensity, do not depend on v_y, and $f(v_x, v_y, v_z) = g_x(v_x) g_y(v_y) g_z(v_z)$, being the g normalized, the integration with respect to this variable is immediately performed, so that the emissivity profile now becomes:

$$j(P, \nu, \mathbf{n}) = \frac{ch B_{12} N}{4\pi} g_x(v_x[\nu]) \times \tag{6}$$

$$\int_\Omega p(\varphi) d\omega' \int_{-\infty}^{\infty} I(\nu'[v_x[\nu], v_z, \nu_o], \mathbf{n}') g_z(v_z) dv_z,$$

where ν and v_x are connected by

$$\nu = \nu_o (1 + \frac{v_x}{c}), \tag{7}$$

since $v_x \equiv v_X$. The advantage of Eq. (6) is that it involves the integration over a velocity component only. We will make use of it, rather than of Eq. (1), every time we will make use of Maxwellian distributions. Note that in this equation the z axis moves while the integration with respect to ω' is performed, and so the z-component of the bulk velocity, w_z, and therefore g_z, change during that integration.

The scattering process is described in Fig. 2 for an exciting radiation whose spectral shape is similar to that of the chromospheric Lyα: the velocity distribution of the coronal scattering ions is represented by circles (isodensity contours). Of the ions of this distribution, only those on the dashed line, whose horizontal coordinate is v_x, can emit at the frequency ν for the observer (Eq. (7)); of these, only the ones which belong to the shaded area are able to absorb a photon and therefore give rise to the emission. The integration over v_z in Eq. (6) is seen, in this figure, as a motion along the shaded portion of the vertical dashed line, during which the position in the exciting spectrum of the absorbed photons changes. Various properties of the scattered line can be deduced from Fig. 2. For example, it is interesting to analyze the particular cases $\varphi = \pi/2, 0, \pi$: in the first case, clearly, the emissivity has the same profile as g_x (ν' independent of v_x), in the second, there is no Doppler shift ($\nu' = \nu$) and the emissivity is given by the product of the exciting intensity times the distribution function g_x; the third case ($\varphi = \pi$) is similar to the second one, except that the exciting line is inverted before multiplying by g_x ($\nu - \nu_o = \nu_o - \nu'$, as Eqs. (3) and (7) show). (The first two cases were pointed out by Beckers & Chipman, 1974.) Let us take a Cartesian system, p, q, r, with the origin in P, the p axis along $\mathbf{n}'$, away from the Sun, and the q axis in the $\mathbf{n}, \mathbf{n}'$ plane (Fig. 3). In general, for a very narrow exciting line at the frequency ν_1 (not necessarily equal to ν_o) and a distribution function f isotropic in velocity space, it is clear from Fig. 3 that, for any $\mathbf{n}'$, the maximum density of scattering ions is found, in velocity space, at the position which corresponds to the minimum distance of the straight line $v_p = c(\nu_1 - \nu_o)/\nu_o = b$ from the center of the velocity distribution function (point A in

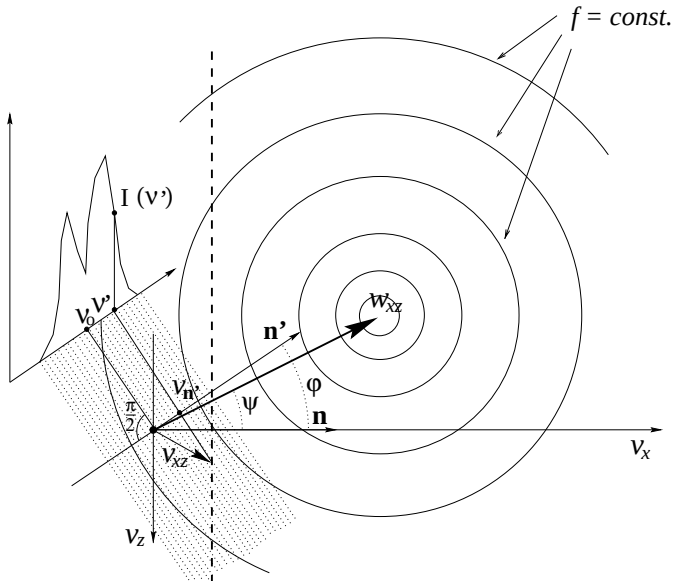

Fig. 2. Scattering process in the $\mathbf{n}, \mathbf{n}'$ plane. The circles are contour plots of the velocity distribution function in the v_x, v_z plane. The intensity of the exciting radiation is represented in the third axis, perpendicular to this plane; only the ions which belong to the shaded area can absorb this radiation.

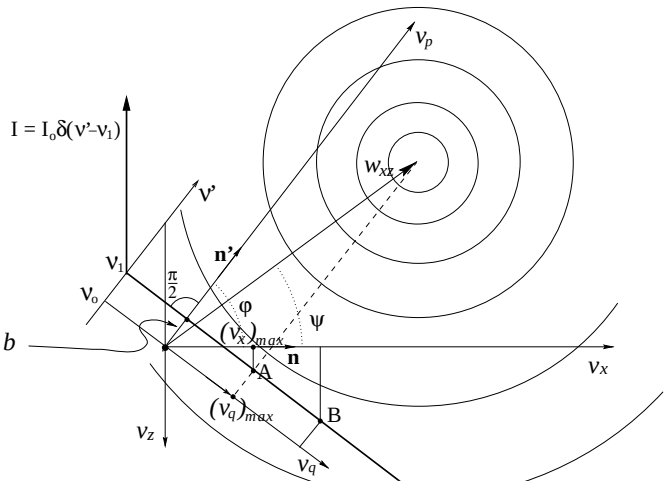

Fig. 3. Scattering process in the v_x, v_z plane. A very narrow exciting line at the frequency ν_1 can be scattered only by the ions on the heavy line. The maximum number of these, per unit velocity, occurs at the point $A \equiv ((v_q)_{max}, b)$. The figure shows also the corresponding v_x coordinate, $(v_x)_{max}$, and the coordinate trasformation from v_q to v_x for a generical point B on the heavy line: $v_x = v_q \sin\varphi + b\cos\varphi$.

Fig. 2). Since $(v_q)_{max} = w_{xz}\sin(\varphi - \psi)$, where w_{xz} is the component of the bulk velocity $\mathbf{w}$ on the v_x, v_z plane and ψ the angle between $\mathbf{w}_{xz}$ and $\mathbf{v}_x$ (positive anticlockwise as seen from $\mathbf{v}_y$), then $(v_x)_{max} = (v_q)_{max}\sin\varphi + b\cos\varphi = w_{xz}\sin(\varphi-\psi)\sin\varphi + b\cos\varphi$. Accordingly, if the exciting line is at the frequency ν_o ($b = 0$), the element of emissivity corresponding to the angle φ is blueshifted for $\varphi > \psi$ and redshifted in the opposite case. In some situations, e. g. radial expansion, ψ is intermediate between the extreme values of φ (for a given P) so that the sum of these elements, e.g. the emissivity, has a small Doppler shift, and the same occurs for the scattered intensity (Eq. (4)). These characteristics will be described, more precisely, in a next section, where we will assume a simple form both for $f(v_x, v_y, v_z)$ and $I(\nu')$.

Note that, given the expression of $v_{n'}$ (Eq. (5)), the last integral of Eq. (6) can be considered a convolution of the functions g_z and I (thought of as a function of v_z).

2.2. Total intensity

The total intensity of the line, e.g. integrated over the profile, is obtained by integration over v_x in Eq. (1) or in Eq. (6). However, if the approximation which allows the use of the latter holds, it is possible to give for it a simpler formula if we refer to the coordinate system p, q, r rather than x, y, z (Fig. 3). The number of photons which have the frequency ν_o in the system where the absorbing ion is at rest, move in the solid angle $d\omega'$ around $\mathbf{n}'$ (in the unit of time and volume) and are absorbed by the ions with velocity components v_p, v_q, v_r, is given by:

$$I(\nu'[v_{n'}, \nu_o], \mathbf{n}')d\omega' \frac{B_{12}}{4\pi} N f(v_p, v_q, v_r) dv_p dv_q dv_r, \qquad (8)$$

where now

$$v_{n'} = v_p.$$

Integration with respect to v_p, v_q, v_r gives the total number of absorptions per unit volume and time, relative to the solid angle $d\omega'$. Since all the absorbed photons are re-emitted in the line, multiplication with the scattering function and integration with respect to ω' gives the total number of photons emitted in the direction $\mathbf{n}$ (towards the Earth observer). Using the factorized form of f, we get, for the integrated emissivity:

$$j(P, \mathbf{n}) = \qquad (9)$$

$$h\nu_o N \frac{B_{12}}{4\pi} \int_\Omega p(\varphi) d\omega' \int_{-\infty}^{\infty} I(\nu'[v_p, \nu_o], \mathbf{n}') g_p(v_p) dv_p$$

(Noci et al. 1987). The evaluation of this expression is a much simpler task, and requires much less computing time, than the integration of Eq. (6) over the frequency.

2.3. Approximate expressions

The region of the coronal spectrum we are mostly interested in is the far/extreme UV. This spectral region is dominated by emission lines produced in part by collisional excitation, in part by radiative excitation from the chromospheric or transition region emission line spectrum. The continuum is negligible in this spectral interval, so that a discrete transition of a coronal ion is excited by a line. This can have a complex shape (generally, for the Lyα line, with two maxima); however, with the purpose of finding a simple expression for the coronal emission, which allow to deduce the properties of an observed spectral line, we approximate, in this section, the spectral shape of the exciting line with a simple function. In the first subsection, which deals

with Maxwellian velocity distributions of the absorbing ions, we will approximate the exciting profile with a Gaussian function, in the second one, which concerns bi-Maxwellian distributions (defined in 2.1), we will need to approximate it with a Dirac δ function, except in a particular case and for the total intensity, where the Gaussian approximation is sufficient.

In the first subsection we will start finding formulae which are quite simple, but involve, still, integration over the direction; to progress further we will assume that the radiation source subtends a very small angle (point source approximation). The accuracy of the analytic expressions that we will obtain in this way will be tested by comparing to numerical calculations.

In the second subsection the point source approximation will be needed from the beginning.

2.3.1. Maxwellian velocity distributions

If the velocity distribution function of the absorbing ions is Maxwellian, we take the axes as in Eq. (6). The analytic integration of this equation is possible with the assumption that the exciting line has a Gaussian shape,

$$I = I_o(\mathbf{n}') \exp(-[\nu' - \nu_1]^2/\sigma_\nu^2(\mathbf{n}'))/\sqrt{\pi}\sigma_\nu(\mathbf{n}'), \tag{10}$$

where ν_1 is the central frequency of the exciting line and σ_ν its e^{-1} half width. The spectral characteristics of the exciting intensity originating in different chromospheric points (points Q, Fig. 1) can be different, hence both I_o and σ_ν depend on $\mathbf{n}'$. The choice of ν_1 not necessarily equal to ν_o has been made to include in this treatment radiative excitation from lines either than the fundamental one, which can be important in some cases (e. g. the O VI line at 1037 Å, Noci et al. 1987).

The use of Eq. (10) makes the integrand of Eq. (6) to be the product of two Gaussian functions. If one calls w_x, w_y, w_z the components of the mean velocity (the second and third of which vary in the course of the integration over direction in Eq. (6)), the evaluation of this equation is easily performed by expressing ν' as a function of v_z through Eqs. (3) and (5). The result is:

$$j(P,\nu,\mathbf{n}) = \frac{chB_{12}}{4\pi} N g_x(v_x) \times$$

$$\int_\Omega I_o(\mathbf{n}') p(\varphi) \frac{(c/\nu_o) e^{-(v_x \cos\varphi - w_z \sin\varphi - b)^2/\sigma'^2}}{\sqrt{\pi}\sigma'} d\omega',$$

where $b = c(\nu_1 - \nu_o)/\nu_o$, as previously defined, and $\sigma'^2 = (q^2 + \sin^2\varphi)V^2$, being $q = \sigma_\nu c/\nu_o V$ and $V = \sqrt{2kT/m}$, with T kinetic temperature. (Note that, if σ_ν depends on the direction, q and σ' are also functions of it.) If we insert the distribution g_x in the integral we get again a product of two Gaussian functions, this time of the variable v_x, and thus the emissivity becomes:

$$j(P,\nu,\mathbf{n}) = \frac{c^2 hB_{12}}{4\pi\nu_o} N \int_\Omega I_o(\mathbf{n}') p(\varphi) \times \tag{11}$$

$$\frac{e^{-(w_x \cos\varphi - w_z \sin\varphi - b)^2/\sigma^2}}{\sqrt{\pi}\sigma} \frac{e^{-(v_x[\nu] - v_o)^2/s^2}}{\sqrt{\pi}s} d\omega'$$

where

$$\sigma^2 = (q^2+1)V^2, \tag{12}$$

$$s^2 = \frac{q^2 + \sin^2\varphi}{q^2+1} V^2, \tag{13}$$

$$v_o = \frac{(q^2 + \sin^2\varphi) w_x + \sin\varphi\cos\varphi\, w_z + b\cos\varphi}{q^2+1}, \tag{14}$$

and v_x is a function of ν according to Eq. (7). Note that, in agreement with the discussion of Sect. 2.1, the case $\varphi = \pi/2$ gives $s = V$, while the extreme cases $\varphi = 0, \pi$ give $s = \sigma_\nu c/\nu_o$, for an exciting line much narrower than the velocity profile, $s = V$ in the opposite case.

The first exponential factor in Eq. (11) affects the total intensity (Doppler dimming), not the profile, since it does not depend on v_x. Taking into account that v_x depends linearly on ν, the second exponential factor (which can not be taken out of the integral because v_o depends on the direction $\mathbf{n}'$) shows that the emissivity has a shape close to Gaussian. Before examining this in more detail we make a further transformation using the quantities $\mathbf{w}_{xz}$ and ψ defined above:

$$w_x = w_{xz}\cos\psi \qquad\qquad w_z = -w_{xz}\sin\psi, \tag{15}$$

($w_{xz} > 0$), so that Eqs. (11) and (14) become

$$j(P,\nu,\mathbf{n}) = \frac{c^2 hB_{12}}{4\pi\nu_o} N \times \tag{16}$$

$$\int_\Omega I_o(\mathbf{n}') p(\varphi) \frac{e^{-[w_{xz}\cos(\varphi-\psi) - b]^2/\sigma^2}}{\sqrt{\pi}\sigma} \frac{e^{-(v_x - v_o)^2/s^2}}{\sqrt{\pi}s} d\omega'$$

and

$$v_o = \frac{\left[q^2\cos\psi + \sin\varphi\sin(\varphi-\psi)\right] w_{xz} + b\cos\varphi}{q^2+1}. \tag{17}$$

Note that the expression of v_o, when compared with that of $(v_x)_{max}$ given in Sect. 2.1, shows the presence of another term, due to the finite width of the exciting line, which contributes to the Doppler shift of a radiatively excited coronal line.

Expression (16) can be evaluated numerically, but its form permits already to deduce important characteristics of a coronal line produced by resonant scattering. It shows that the element of emissivity corresponding to the angle φ has a Gaussian shape whose width and position are given, on a velocity scale, by Eqs. (13) and (17), respectively. The spectral shape of the emissivity, resulting from the integration over direction, is the addition of these elementary functions having different width and, if w_{xz} or b are not zero, different position. Numerical calculations show that the spectral shape of the emissivity is quite close to Gaussian, which suggests to keep constant the integrand of Eq. (16), i. e. to adopt the point source approximation. Therefore Eqs. (16), (13) and (17) take the simpler forms

$$j(P,\nu,\mathbf{n}) = \frac{c^2 hB_{12}}{4\pi\nu_o} N F p(\phi) \times \tag{18}$$

$$\frac{e^{-[w_{rn}\cos(\phi-\psi)-b]^2/\sigma^2}}{\sqrt{\pi}\sigma}\,\frac{e^{-(v_x[\nu]-v_o)^2/s^2}}{\sqrt{\pi}s},$$

$$s^2=\frac{q^2+\sin^2\phi}{q^2+1}V^2 \tag{19}$$

and

$$v_o=\frac{\left[q^2\cos\psi+\sin\phi\sin(\phi-\psi)\right]w_{rn}+b\cos\phi}{q^2+1}, \tag{20}$$

where $F=\int_\Omega I_o d\omega'$ is the total flux from the source in the exciting line, ϕ the position angle, already defined (Fig. 1), w_{rn} the component of **w** in the **r, n** plane, ψ the angle between $\mathbf{w}_{rn}$ and **n**, and the function $v_x(\nu)$ is given by Eq. (7). If σ_ν changes with the direction, one needs here, to calculate q and σ, an average value. Note that we have not assumed radial expansion.

These equations are very useful for first approximation calculations. In particular, let us consider the width and wavelength position of a coronal line, which are observable quantities and depend on the spectral characteristics of the emissivity of all the plasma elements along the line of sight. To understand which information give us Eqs. (19) and (20), which concern the emissivity, on these quantities, we first examine their accuracy by comparison with emissivity numerical calculations, and then, under a) and b) below, we discuss the effect of the integration along the line of sight.

We start with Eq. (19). The emissivity calculations of Beckers and Chipman (1974), for the Lyα line, assume point source and radial expansion, and use the chromospheric Lyα profile given by Bruner & Rense (1969), therefore the comparison concerns only the Gaussian approximation for the profile of the exciting line. The e^{-1} half width of this, to be used in Eqs. (19) and (20), is obtained from the full width at half maximum of the scattered line, in the limiting case $\phi=\pi, T=\infty$, which is given by Beckers and Chipman (0.84 Å). In the case of no solar wind the result, for $T=1.4\times10^6K$, is that Eq. (19) is in error by 12% at $\phi=0,180^o$, by less than 3% at $\phi=20^o,160^o$, by less than 1% at $\phi=70^o,110^o$. At $\phi=90^o$ the comparison looses interest because Eq. (19) gives the correct result, as shown in Sect. 2.1, for the Beckers & Chipman assumptions (point source and Maxwellian velocity distribution). The differences are the same for the solar wind case (up to 300 km/sec) except for $\phi=0,180^o$. For these limiting values, as explained in Sect. 2.1, the way the emissivity profile is obtained from the intensity of the exciting radiation does not involve integration, but rather a multiplication with the distribution function of the velocity component along the line of sight, v_x, of the absorbers. Hence the scattered line has an asymmetric shape because this multiplication weights differently the two peaks of the chromospheric Lyα.

Another comparison concerning Eq. (19) has been made with the numerical integrations of Withbroe et al. (1982) and of Ventura & Spadaro (1998), which also refer to the Lyα line but use the Gouttebroze et al. (1978) profile. (We have used the full width at half maximum given by Ventura and Spadaro, 0.66 Å). This comparison is more significant because these authors have not made the point source approximation, and thus the check is a test also of this approximation. The comparison with the calculations of Withbroe et al. (1982), which concern no solar wind and $T=1.5\times10^6K$, made for the position angle ϕ in the interval 15^o-175^o, shows that the error of Eq. (19) is only a few percent, not only for large values of ρ (ρ is the distance of the line of sight from Sun center, and $\rho=\infty$ corresponds to the point source approximation), but also for low values of it, being still less than 10% at $\rho=1.1r_\odot$ and $\phi=90^o$, where the extreme values of the scattering angle differ considerably from ϕ. The accuracy of Eq. (19) decreases when the solar wind velocity is not zero, for two reasons: (i) the dependence of v_o on φ when the outflow speed is not zero (we refer to Ventura & Spadaro (1998) for a discussion of this effect); (ii) the fact that, for large solar wind speeds, the velocity distribution function of the absorbing ions overlaps only the wing of the exciting intensity profile, where the Gaussian approximation may be particularly in error (but also the 'exact' calculation, for the larger importance of the measurement errors on the observed profile). In spite of this, the accuracy of Eq. (19) is still good, as the comparison with Ventura & Spadaro (1998) shows, for outflow velocities up to 500 km/sec, the difference with numerical calculations being of the order of 10% or less, except for $\phi=90^o$ and $w=500$ km/sec, when it reaches $\simeq 24\%$. (Ventura & Spadaro (1998) assumed radial outflow $\rho=2r_\odot$, $T=1.41\times10^6K$, $\phi=30^o,60^o,90^o$, and rather large solar wind velocities (≥ 316 km/sec), being interested mainly in the effects of the velocity on the radiatively excited lines of a CME.)

Another important observable quantity is the Doppler shift; we have examined how good is Eq. (20) to give the emissivity Doppler shift, by comparing it with the numerical calculations of Beckers & Chipman (1974) and Ventura & Spadaro (1998) (no calculations of Doppler shift are given by Withbroe et al. 1982). The differences between Eq. (20) and the results of Beckers & Chipman, using $\phi=\psi$ (radial solar wind) and $\nu=\nu_1$, are less than 25% at $\phi=0,180^o$ and $\phi=45^o,135^o$, for outflow speeds up to 200 km/sec; they are larger ($\simeq 35\%$) for outflow speed of 300 km/sec. These differences are essentially due to effect (ii) described above. Like Eq. (19), Eq. (20) gives the exact result at $\phi=90^o$ ($v_o=w_{rn}\cos\psi$) for the assumptions of Beckers & Chipman (1974).

The comparison of Eq. (20) with the results of Ventura & Spadaro (1998), for radial expansion, shows a difference $\lesssim 30\%$, and often in the 15% range, at $\phi=30^o$ and $\phi=60^o$, for solar wind speeds up to 630 km/sec, and no difference at $\phi=90^o$ ($v_o=0$). If **w** is parallel to **n**, the difference is $\lesssim 20\%$ for the same angles and solar wind speeds ($\lesssim 4\%$ for $\phi=90^o$). The difference must decrease for heliocentric distances larger than the one considered by Ventura & Spadaro ($\rho=2r_\odot$) when the differences $|\varphi-\psi|$ become smaller and smaller.

We conclude that Eqs. (19) and (20) are quite good, particularly the first one, for first approximation calculations, for Maxwellian velocity distributions.

Having established a level of accuracy for these equations, which concern the emissivity, we now try to deduce the char-

acteristics of an observed line, i.e. the effect of the integration along the line of sight.

a) *Spectral shape and Doppler shift of the scattered line*

According to the previous discussion, for lines of sight above $\rho \simeq 2r_\odot$ Eq. (19) is essentially correct for the emissivity width. The integration along the line of sight involves the contribution of plasma elements having ϕ decreasing from π, at $x = -\infty$, to 0, at $x = \infty$. The maximum value of the emissivity width occurs on the plane of the sky $(s = V)$; for $\phi = 60^o$, i.e. $x = 0.577\rho$ and $r = 1.15\rho$, Eq. (19) gives $s = 0.91V$ (using Gouttebroze et al. (1978) profile to calculate q). Since the plasma elements closer than 0.577ρ to the plane of the sky possess generally the largest density, we conclude that the width difference between a collisionally excited and a radiatively excited line is usually relatively small, the radiatively excited line being narrower. This is true if the bulk velocity and b are zero; otherwise one should take into account the fact that the various plasma elements along the line of sight have their emissivities at different positions on the frequency axis, since v_o is not constant along the line of sight. This can make a radiatively excited line wider than if the mechanism of excitation were collisional. (This effect is similar, but not the same, to the one caused by the dependence of v_o on φ, see Eq. (17), mentioned above and discussed by Ventura and Spadaro (1998)).

In conclusion, dense structures away from the plane of the sky and flows have opposite effects on the line width; their importance depends on the density and velocity distributions. These possible effects should be taken into account when interpreting the observations.

Let us consider the Doppler shift. The first term on the right hand side of Eq. (20), independent of the scattering angle, for radial outflow ($\psi = \phi$) contributes with a blueshift for plasma elements in front of the plane of the sky, with a redshift in the opposite case, and does not give contribution for plasma elements on the plane of the sky. Similarly behaves the third term, $b\cos\phi$, while the second, containing the factor $\sin(\phi - \psi)$, is, for radial outflow, zero. Hence, the contributions of the various plasma elements along the line of sight, for what concerns the Doppler shift, tend to cancel. We conclude that a radiatively excited line produced in a radially expanding plasma, as that of a halo coronal mass ejection (CME), is characterized by a small Doppler shift.

For non-radial outflow the shift is larger; for example, if $\psi = 0$ for all plasma elements (motion along the line of sight towards the Earth, $w_{rn} = w_x$),

$$v_o = \frac{\left[q^2 + \sin^2\phi\right] w_x + b\cos\phi}{q^2 + 1},$$

which shows that, if $\nu_1 = \nu_o$, all the plasma elements on the line of sight contribute with a blue shifted emission. The resulting shift of the emerging line will be somewhat smaller than w_x, in velocity units.

In any case an accurate modelling is needed to interpret the Doppler shifts observed in a complex expanding structure.

The fact that v_o is different from w_x has an interesting consequence: it implies that Doppler shift and velocity, for a radiatively excited line, are not connected by the usual formula

$$\Delta\lambda = \lambda w_x/c$$

but, rather, by the expression:

$$\Delta\lambda = \lambda v_o/c.$$

The two coincide for $\phi = \pi/2$, which means that the use of the former causes a small error if the density of the emitters close to the plane of the sky is dominant, but can give quite different results if this is not true.

This behaviour of the radiatively excited component of a line causes a separation from the collisional component. The emissivity of the latter will indeed be shifted proportionally to w_x and therefore it will be separated from the emissivity of the radiative component by $\delta\lambda = \lambda(w_x - v_o)/c$. This effect might give two separated lines; if so, it might lead to the determination of w_z or ϕ. However, if the separation is large enough to produce two distinct lines, the coronal absorption profile is shifted out of the chromospheric line and therefore the radiative component is strongly depressed. Thus it appears that this effect might be observable only with the H I Lyα line, where the radiative component is much larger than the collisional one, and therefore even a large suppression of the former, caused by a large $w_x - v_o$ difference, can leave the two components of similar intensity.

Obviously the same information on $w_x - v_0$ colud be obtained with two different nearby lines, one collisionally, one radiatively excited.

b) *Doppler dimming*

The first exponential factor of Eq. (16) shows how the emissivity of a spectral line radiatively excited from a line spectrum is depressed if $w_{xz}\cos(\varphi - \psi) - b \neq 0$. As noted in the Introduction, calculations concerning this phenomenon (Doppler dimming) have been published by Hyder & Lites (1970), Beckers & Chipman (1974), Kohl & Withbroe (1982), Withbroe et al. (1982), Noci et al. (1987). The use of the point source approximation permits a very simple evaluation of this effect. Integrating over v_x in Eq. (18) one gets, for the total emissivity:

$$j(P, \mathbf{n}) = \frac{chB_{12}}{4\pi} Np(\phi) \frac{e^{-[w_{rn}\cos(\phi-\psi)-b]^2/\sigma^2}}{\sqrt{\pi}\sigma} F,$$

which is particularly simple for radial outflow ($\psi = \phi$) and exciting line with its center at the frequency of the transition ($b = 0$). It is needless to say that, for $b > 0$, this equation includes the case of Doppler pumping. This equation allows very easily first approximation calculations.

2.3.2. Bi-Maxwellian velocity distributions

In this section we will work out an expression for the emissivity due to resonant scattering, which can be applied to velocity distributions with different widths in the radial and perpendicular directions, and therefore can be used to interpret the most recent coronal observations which show that the ions in coronal holes have this kind of velocity distribution (Kohl et al. 1997). In this case Eq. (6) can not be used and in Eq. (1) the form of the function f is rather complicated, which makes that equation difficult to handle analytically (see, e. g., Li et al. 1998). Therefore we will limit ourselves to the point source approximation and choose the axes as in Sect. 2.2, so that we can put $f = g_p(v_p)g_q(v_q)g_r(v_r)$ $(v_p = v_\parallel,\ v_q^2 + v_r^2 = v_\perp^2)$, being the g normalized.

a) *Profile*

To obtain a simple expression for the line profile we need to assume also, beyond a point source of radiation, that the width of the exciting line is much smaller than that of the velocity distribution function of the absorbing ions,

$$I(\nu', \mathbf{n}') = I_o(\mathbf{n}')\delta(\nu' - \nu_1), \tag{21}$$

$\delta(\nu' - \nu_1)$ being the Dirac function. Hence the integration of expression (8) with respect to v_p, v_r, considering that $v_p = c(\nu' - \nu_o)/\nu_o$ (Eq. (3)), gives

$$(c/\nu_o)(B_{12}/4\pi)Ng_q(v_q)dv_q d\omega' I_o(\mathbf{n}')g_p(b),$$

where $b = c(\nu_1 - \nu_o)/\nu_o$ as in the previous section, for the number of photons moving in the solid angle $d\omega'$ in the unit of time and volume, absorbed by the ions with velocity components along q between v_q and $v_q + dv_q$. The emissivity, then, is given by:

$$j(P, \nu, \mathbf{n})d\nu =$$

$$hc\frac{B_{12}}{4\pi}Fp(\phi)N\frac{e^{-(b-w_\parallel)^2/V_\parallel^2}}{\sqrt{\pi}V_\parallel}\frac{e^{-(v_q-w_q)^2/V_\perp^2}}{\sqrt{\pi}V_\perp}dv_q,$$

where we have introduced some symbols from Sect. 2.1, and w_q is the component of **w** on the q axis. Given the assumption on the width of the exciting line, v_x (and therefore ν) is now a function of the component v_q only, $v_x = v_q \sin\varphi + b\cos\varphi$ (Fig. 3), i. e., in the point source approximation, $v_x = v_q \sin\phi + b\cos\phi$. Therefore we can write:

$$j(P, \nu, \mathbf{n}) = hc^2\frac{B_{12}}{4\pi\nu_o}p(\phi)FN \times \tag{22}$$

$$\frac{1}{\pi V_\parallel V_\perp \sin\phi}e^{-(b-w_\parallel)^2/V_\parallel^2}e^{-(v_x[\nu]-v_o)^2/V_\perp^2\sin^2\phi},$$

where v_x is a function of ν according to Eq. (7), and v_o is the quantity given by Eq. (20) for a very narrow exciting line ($q = 0$).

This equation shows, again, that there is no Doppler shift if the outflow is radial and the exciting line at ν_o. Doppler dimming (first exponential factor) depends on the width of the parallel velocity distribution, while the perpendicular distribution and the scattering angle are responsible of the width of the emitted line. The effect of the $\sin\phi$ factor on this width appears to be larger than in the case of the Maxwellian distribution, see Eq. (19), but this is, presumably, only the effect of the approximation of a very narrow exciting line, because, in this case, Eq. (19) gives the same dependence of the width on the scattering angle as Eq. (22).

Eq. (22) can be useful being very simple. However, the error introduced by the simplifying assumptions (very narrow exciting line and point source approximation) is not small. The latter approximation, in particular, assumes the width of the velocity distribution function of the absorbers to be $V_\parallel$ for any φ, while, in reality, it is intermediate between $V_\parallel$ and $V_\perp$, except when $\mathbf{n}'$ and $\mathbf{r}$ are parallel. Hence Eq. (22) should be used with caution, particularly at small heliocentric distances. This effect, for what concerns its influence on the intensity ratio of the OVI resonance doublet, is discussed by Li et al. (1998) and by Dodero et al. (1998).

In the limit $\phi = \pi/2$ one can obtain a simple equation with a greater level of validity. Indeed in this case assumption (21) is not necessary to make v_x independent of $v_p(= v_\parallel)$, so that the integration of Eq. (8) gives:

$$j(P, \nu, \mathbf{n}) = hc\frac{B_{12}}{4\pi}NFp(\pi/2)\frac{1}{\pi V_\parallel V_\perp}\times$$

$$e^{-(v_x-w_x)^2/V_\perp^2}\int_{-\infty}^{\infty}P(\nu'[v_\parallel, \nu_o])e^{-[v_\parallel-w_\parallel]^2/V_\parallel^2}dv_\parallel,$$

where w_x is the bulk velocity along the line of sight, and P is the profile of the exciting radiation, $P = I/I_o$. If P is Gaussian, according to Eq. (10), the integration gives:

$$j(P, \nu, \mathbf{n}) = hc^2\frac{B_{12}}{4\pi\nu_o}\times$$

$$NFp(\pi/2)\frac{e^{-(b-w_\parallel)^2/\sigma_\parallel^2}}{\sqrt{\pi}\sigma_\parallel}\frac{e^{-(v_x-w_x)^2/V_\perp^2}}{\sqrt{\pi}V_\perp},$$

where $\sigma_\parallel^2 = V_\parallel^2\left[\left(\frac{\sigma_\nu c}{\nu_o V_\parallel}\right)^2 + 1\right]$. Since also this equation is based on the point source approximation, the *caveat* of last paragraph holds also here.

b) *Total intensity*

For the total intensity it is possible to obtain an expression with a considerably greater accuracy than one would obtain by integrating Eq. (22) over the frequency. It is still necessary to retain the point source approximation but not that of a very narrow exciting line. Since all absorbed photons contribute to the total intensity, we need simply to calculate the absorptions as in Sect. 2.2. For these, in the point source approximation, only

the ion velocity distribution in the parallel direction matters, hence the integrated emissivity is obtained, quite simply, from Eq. (9):

$$j(P,\mathbf{n}) = h\nu_o \frac{B_{12}}{4\pi} NFp(\phi) \int_{-\infty}^{\infty} P(\nu'[v_\parallel,\nu_o]) g_\parallel(v_\parallel) dv_\parallel,$$

where we have put $v_\parallel$ for v_p. This, for a Gaussian shape of the exciting line, whose central frequency is ν_1, becomes:

$$j(P,\mathbf{n}) = hc \frac{B_{12}}{4\pi} NFp(\phi) \frac{e^{-(b-w_\parallel)^2/\sigma_\parallel^2}}{\sqrt{\pi}\sigma_\parallel},$$

where $\sigma_\parallel$ is the quantity defined above. This also is a very simple expression, but we remind, again, that it assumes the absorbing profile to have the width $V_\parallel$ for all directions $\mathbf{n}'$.

3. Scattering by free electrons

Let us consider the scattering of a photon from the direction $\mathbf{n}'$ to the direction $\mathbf{n}$, operated by a free electron at the point P (Fig. 1). The probability of this process is described by a cross section σ (Thomson cross section), having the constant value 0.66524×10^{-24} cm^2, and a geometrical factor $p_e(\varphi)$, which represents the probability of a deflection through an angle φ, with the expression:

$$p_e(\varphi) = \frac{3}{4} \frac{1+\cos^2\varphi}{4\pi}$$

(Chandrasekhar 1950; Landi Degl' Innocenti 1984). To get the emissivity we can argue as in Sect. 2.1, but since, in this case, the scattering particles do not have a fixed frequency of operation, i.e. they can scatter photons with frequency different from ν_o, to get the emissivity at ν (in the observer frame, S'), we need to vary v_x and ν_o keeping ν fixed, thus considering photons that are seen with a different frequency by the scattering electron but have the same frequency for the observer. In other words, the emissivity of Eqs. (1) and (6) becomes infinitesimal, as well as the transition probability B_{12}, which becomes proportional to the frequency interval $d\nu_o$; hence one needs to integrate with respect to v_x, with ν constant, once ν_o is expressed as a function of v_x via Eq. (7). However, it is simpler to use, instead of this procedure, the argument used by van Houten (1950), which is based on the calculation of the total frequency shift of a photon, caused by the scattering. Following van Houten we choose rectangular coordinates, ξ, η, ζ, such that $\eta \equiv y$ and ξ is the bisector of the scattering angle (φ). The velocity components along $\mathbf{n}$ and $\mathbf{n}'$ are then given by:

$$v_{n'} = v_\xi \cos(\varphi/2) - v_\zeta \sin(\varphi/2),$$

$$v_n = v_\xi \cos(\varphi/2) + v_\zeta \sin(\varphi/2).$$

A photon which has the frequency ν_o in the electron frame (S) has the frequency $\nu' = \nu_o(1 + v_{n'}/c)$ in S' when it is emitted from the solar surface. The frequency ν_o remains unchanged in S after the scattering, but it changes to $\nu = \nu_o(1 + v_n/c)$ for the Earth observer. The total frequency shift is, therefore:

$$\nu - \nu' = \nu_o(v_n - v_{n'})/c = (\nu_o/c) 2 v_\zeta \sin(\varphi/2),$$

which shows that the velocity component along ξ does not produce a frequency shift. Hence the intensity at the frequency ν is due to contributions from all the frequencies ν' in the spectrum emitted by the source, each one weighted by the number of electrons which produce the shift $\nu - \nu'$, i.e. those wich have the ζ component of the velocity in the interval $v_\zeta, v_\zeta + dv_\zeta$. Therefore:

$$j(P,\nu,\mathbf{n}) = \sigma N_e \int_\Omega p_e(\varphi) \times \tag{23}$$

$$d\omega' \int_{-\infty}^{\infty} I(\nu' = \nu - \Delta\nu, \mathbf{n}') f_{n'}(v_\xi, v_\eta, v_\zeta) dv_\xi dv_\eta dv_\zeta,$$

where $f_{n'}$ is the velocity distribution function of the electrons and

$$\Delta\nu = 2 v_\zeta \sin(\varphi/2) \nu_o / c.$$

Given the choice of the axes, the function $f_{n'}$ can change with the direction $\mathbf{n}'$, and furthermore ν_o, which is the frequency of a scattered photon in the electron frame, depends on v_n, once ν is given, hence $\Delta\nu$ depends on v_ξ, v_ζ. To simplify the expression of the emissivity we assume the velocity distribution function to be Maxwellian and we notice that $v_n, v_{n'} \ll c$, which makes the differences among the frequencies ν, ν' and ν_o small compared with the frequencies themselves. Hence ν_o can be substituted with ν in the last equation, and thus $\Delta\nu$ becomes a very simple function of the velocity component v_ζ only,

$$\Delta\nu = 2 v_\zeta \sin(\varphi/2) \nu / c. \tag{24}$$

Accordingly, Eq. (23) becomes:

$$j(P,\nu,\mathbf{n}) = \tag{25}$$

$$\sigma N_e \int_\Omega p_e(\varphi) d\omega' \int_{-\infty}^{\infty} I(\nu' = \nu - \Delta\nu[v_\zeta], \mathbf{n}') g_\zeta(v_\zeta) dv_\zeta,$$

where $\Delta\nu$ depends on v_ζ through Eq. (24).

3.1. Visible radiation

If we apply Eq. (25) to the continuum photospheric spectrum, since $\Delta\nu \ll \nu$, we can put $I(\nu') = I(\nu)$, which gives the known expression:

$$j(P,\nu,\mathbf{n}) = \sigma N_e \int_\Omega p_e(\varphi) I(\nu,\mathbf{n}') d\omega',$$

where the dependence on $\mathbf{n}'$ is brought about by limb darkening.

Let us consider a photospheric absorption line, that we approximate with the Dirac function, which is justified by the large width of the electron velocity distribution. Since $\nu' = \nu - \Delta\nu$, we write:

$$I(\nu',\mathbf{n}') = I_c(\mathbf{n}') - I_o(\mathbf{n}') \delta(\nu - \Delta\nu - \nu_1),$$

where I_c is the intensity of the photospheric continuum and ν_1 the frequency at the center of the absorption line. If we integrate Eq. (25), changing the variable from v_ζ to $\Delta\nu$ through Eq. (24), we get:

$$j(P,\nu,\mathbf{n}) = \sigma N_e J_c -$$

$$\sigma N_e \int_\Omega p_e(\varphi) I_o(\mathbf{n}') g_\zeta(v'_\zeta) \frac{c}{2\nu\sin(\varphi/2)} d\omega',$$

where $v'_\zeta = c(\nu-\nu_1)/2\nu\sin(\varphi/2)$ and $J_c = \int_\Omega p_e(\varphi) I_c(\mathbf{n}') d\omega'$. A Maxwellian distribution gives:

$$j(P,\nu,\mathbf{n}) = \sigma N_e J_c - \sigma N_e \int_\Omega p_e(\varphi) I_o(\mathbf{n}') \times \tag{26}$$

$$\frac{c}{2\nu\sin(\varphi/2)} \frac{1}{\sqrt{\pi}V_e} e^{-\left[\frac{\nu(1-2\sin(\varphi/2)w_\zeta/c)-\nu_1}{2\sin(\varphi/2)V_e\nu/c}\right]^2} d\omega',$$

where $V_e = \sqrt{2kT_e/m_e}$, being T_e the temperature of the electrons and m_e their mass, and w_ζ, the component of the bulk velocity on the ζ axis, varies with $\mathbf{n}'$. This result shows that the photospheric line is changed, by the scattering process, in an absorption line with a width similar to the width of the velocity distribution function. The difference is caused by the factor $2\sin(\varphi/2)$ (van Houten 1950), whose effect is an increase of about $\sqrt{2}$, if the largest density, along the line of sight, is on the plane of the sky. The observation of absorption lines in the visible coronal spectrum can lead to the determination of T_e (Grotrian 1931). However, given the low mass of the electrons, the width of the coronal line is so much larger than that of the exciting line that the intensity reduction at the line center in the coronal spectrum is small and therefore the accuracy of the determination low.

3.2. The Ly-α line

Hughes (1965) suggested to determine the coronal electron temperature by observing the Lyα line produced by the coronal free electrons which scatter the chromospheric Lyα. As mentioned in the Introduction, the difficulty is again the weakness of the line, in particular with respect to the resonantly scattered component, which is superimposed on it, but the UVCS instrument on SOHO might be able to accomplish the measurement (Noci et al. 1997).

For the emissivity of this line an expression similar to Eq. (26) holds:

$$j(P,\nu,\mathbf{n}) = \sigma N_e \int_\Omega p_e(\varphi) I_o(\mathbf{n}') \times \tag{27}$$

$$\frac{c}{2\nu\sin(\varphi/2)} \frac{1}{\sqrt{\pi}V_e} e^{-\left[\frac{\nu(1-2\sin(\varphi/2)w_\zeta/c)-\nu_1}{2\sin(\varphi/2)V_e\nu/c}\right]^2} d\omega'.$$

This equation shows that the dependence of the element of emissivity on the scattering angle is larger than in the case of resonant scattering, and thus the emissivity is the sum of Gaussian contributions of considerably different width. For example, at $\rho = 2r_\odot$, on the plane of the sky, φ changes from 60^o to 120^o so that the widths of the emissivity elements change from $V_e\nu/c$ to $1.7V_e\nu/c$. According to Withbroe et al. (1982), if $\rho \gtrsim 2r_\odot$ the width of the emissivity profile differs by less than 5% from the one which obtains from the point source approximation:

$$s_e = 2V_e \sin(\phi/2)\nu/c, \tag{28}$$

but the difference becomes larger for smaller values of the heliocentric distance, reaching $\simeq 15\%$ at $\rho = 1.1r_\odot$ for $\phi \lesssim \pi/2$.

Taking the value given by Eq. (28) as representative of the e^{-1} half width of the emissivity of this line, we note that it is larger than the thermal width for position angles larger than $\pi/3$, up to a factor of two for $\phi = \pi$. In the case $\phi = \pi/2$ the e^{-1} half width is $\sqrt{2}V_e\nu/c$. For small position angles the width of the emissivity becomes much smaller than the width of the velocity distribution function. In the limit $\phi = 0$ one would obtain a zero width, but the approximations leading to Eq. (28) are not valid in this case. This is immediately seen from Eq. (27), where $\Omega > 0$. Furthermore, even in the limiting case of the scattering angle $\varphi = 0$, Eq. (24) gives $\Delta\nu = 0$ and, therefore, $\nu = \nu'$. Accordingly, Eq. (23) yields:

$$dj(P,\nu,\mathbf{n}) = \sigma N_e p_e(0) d\omega' I(\nu),$$

i.e. the contribution to the emissivity relative to the scattering angle $\varphi = 0$ has the same profile as the exciting line, which means that the width of the exciting line is a lower limit to the width of the scattered line.

One can then use the point source approximation for the emissivity, for $\rho \gtrsim 2r_\odot$, to calculate the emerging intensity. This deviates somewhat from a Gaussian shape because the variation of ϕ, and therefore of the emissivity width, along the line of sight, causes non-Gaussian wings to be present for any ρ (Hughes 1965, Withbroe et al. 1982).

It is interesting to consider the effect of a dense feature localized at some value of ϕ. Since the emissivity maximum at $\nu = \nu_1$ increases when the angle ϕ decreases, the best conditions for the observation of the line occur for structures (like streamers) outside the plane of the sky, towards the observer.

Finally, we like to note that the center of the scattered line is shifted from ν_1: the emissivity relative to the scattering angle φ has its center at $\nu_1[1+2(w_\zeta/c)\sin(\varphi/2)]$. The shift is negligible, since the bulk speeds present in the solar corona (w_ζ) are much smaller than V_e.

4. Conclusions

We have given expressions for the spectral shape of the radiation scattered by the coronal ions, and applied them to simple cases, for what concerns the ion velocity distribution, the spectrum of the radiation which excites the coronal emission and the angular extent of the source. The one which corresponds to the assumption of a Maxwellian velocity distribution of the ions, and to an exciting spectrum consisting of an emission line with a Gaussian shape gives the most useful formulae for the

intensity profile of the emissivity of the coronal line, and, in particular, for its spectral shift and width. The dependence of these two quantities on the position angle of the scattering plasma element, the width of the exciting line and the mean velocity of the coronal ions, which result from those formulae, had not been clearly understood in the past.

We have also given expressions for the case of a bi-Maxwellian velocity distribution of the absorbing ions, and for the electron scattered Lyα line.

We have discussed the accuracy of the simple formulae obtained.

The results of this paper will be useful for the interpretation of the spectrum of the extended solar corona.

Acknowledgements. We like to thank the referee for his suggestions to improve the clearness of the paper. This work was supported in part by Agenzia Spaziale Italiana.

References

Altschuler M.D., Perry R.M., 1972, Solar Phys. 23, 410.
Beckers J.M., Chipman E., 1974, Solar Phys. 34, 151.
Bruner, E. C. and Rense, W. A., 1969, ApJ 157, 417.
Chandrasekhar S., 1950, Radiative Transfer, Clarendon Press, Oxford.
Dodero M. A., Antonucci A., Giordano S., Martin R., 1998, Solar Phys. (in press).
Gabriel A.H., Garton W.R.S., Goldberg L. et al., 1971, ApJ 169, 595.
Gouttebroze P., Lemaire P., Vial J. C., Artzner G., 1978, ApJ 225, 655.
Grotrian W., 1931, Z. f. Ap. 3, 199.
Hughes C. J., 1965, ApJ 142, 321.
Hyder C.L., Lites B.W., 1970, Solar Phys. 14, 147.
Kohl J.L., Noci G., Antonucci E. et al., 1997, Solar Phys. 175, 613.
Kohl J.L., Withbroe, G.L., 1982, ApJ 256, 263.
Landi Degl' Innocenti E., 1984, Solar Phys. 91, 1.
Li X., Habbal S.R., Kohl J.L., Noci G., 1998, ApJ 501, L133.
Noci G., Kohl J.L., Antonucci, E. et al., 1997, ESA SP-404, 75.
Noci G., Kohl J.L., Withbroe G.L., 1987, ApJ 315, 706.
Olsen E.L., Leer E., Holzer T.E., 1994, ApJ 420, 913.
Raymond J.C., Kohl J.L., Noci G. et al., 1997, Solar Phys. 175, 645.
van de Hulst H.C., 1950, Bull. Astr. Inst. Netherlands 11, 135.
van Houten C.J., 1950, Bull. Astr. Inst. Netherlands 11, 160.
Ventura R., Spadaro D., 1998, A&A, this issue.
Withbroe G.L., Kohl J.L., Weiser H., Munro, R.H., 1982, Space Sci. Rev. 33, 17.